TITLE: Thermoelastic Analysis For A Thick Plate Under The Radiation Boundary Conditions

AUTHORS: G DHAMEJA,L KHALSA,Vinod VARGHESE

PAGES: 35-44

ORIGINAL PDF URL: https://dergipark.org.tr/tr/download/article-file/2629726

Research Article

Thermoelastic Analysis For A Thick Plate Under The Radiation Boundary Conditions

[1]G. Dhameja 🆔, [2]L. Khalsa 🆔, [3]*V. Varghese 🆔

[1,2,3] Department of Mathematics, M.G. College, Armori, Gadchiroli, India
E-mails: [1]dhameja.geeta0311@gmail.com, [2]lalsinghkhalsa@yahoo.com, [3]*vino7997@gmail.com

Abstract

A fractional Cattaneo model for studying the thermoelastic response for a finite thick circular plate with source function is considered. The thick plate is subjected to radiation-type boundary conditions on the upper and lower surfaces, and its curved surface is kept at zero temperature. The theory of integral transformations is used to solve the generalized fractional Cattaneo-type, classical Cattaneo-Vernotte and Fourier heat conduction model. The analytical expressions of displacement components using thermoelastic displacement potentials; and thermal-stress distribution are computed and depicted graphically. The effects of the fractional-order parameter and the relaxation time on the temperature fields and their thermal stresses are investigated. The findings show that the higher the fractional-order parameter, the higher the thermal response. The greater the relaxation period, the longer the heat flux propagates on thick structures.

Keywords: *Fractional Cattaneo-type equation; fractional calculus; non-Fourier heat conduction; thick plate; thermal stress; integral transform.*

1. Introduction

It is required to preserve the structural elements from wear, corrosion, and delamination in high-temperature environments such as the cosmos, thermal power stations, and internal combustion engines. These kinds of environments have incredibly high temperatures. The development of functionally graded materials has been done to alleviate the effects of thermal and residual stresses. Functionally graded materials can avoid destruction because of the gradual change in the material properties. Recently, Haskul [1,2] obtained analytical solutions for the stresses and displacements of a functionally graded cylindrically curved beam subjected to a heat load in the radial direction using von Mises' yield criterion. Haskul et al. [3,4] investigated the elastic stress response of a thick-walled cylindrically curved panel subjected to a radial temperature gradient under the assumption of generalized plane strain according to both yield criteria, Tresca and von Mises.

As everyone knows, the heat current is based on particles or quasi-particle motion from the macroscopic experience. The same reflects in Fourier's law within the framework of the classical parabolic heat conduction equation in which the velocity of heat transport is not limited. A modified Fourier's law fulfilled these conditions explicitly by considering the finite propagation velocity of heat in the conduction equation by the so-called hyperbolic heat conduction equation. Furthermore, technological development with advancements in Science helps to revolutionize by introducing the heat relaxation time to the non-equilibrium heat conduction mechanism [5-8]. Cattaneo [9] and Vernotte [10] multiplied the thermal relaxation time to a partial time derivative of the

heat flux. This so-called Cattaneo-Vernotte hyperbolic heat conduction equation can predict the non-equilibrium heat conduction progression combined with the energy equation. Meanwhile, Compte and Metzler [11] proposed four possible generalizations of the Cattaneo telegraph equation. Though the theoretical modeling of Cattaneo-Vernotte equations overcomes the infinite heat propagation speed for the non-equilibrium process, few nonconformities in the experimental results were noticed by Jiang et al. [12].

Povstenko [13] proposed a quasi-static uncoupled theory of thermoelasticity based on a fractional heat conduction equation. Povstenko [14] published highly cited literature reviews on fractional thermoelasticity. The above literature emphasizes that coupling between deformation and heat conduction in the heat equation into account does not complicate the Neumann boundary value problem in the quasi-static theory framework. In the framework of fractional thermoelasticity, Povstenko [15] also proposed the time-fractional Cattaneo heat conduction equation from the time-non-local generalization of the Fourier law using different kernels, i.e., Mittag-Leffler type, within the framework of corresponding thermal stress theory. Mishra and Rai [16] obtained the fractional single-phase-lagging heat conduction model by applying the fractional Taylor series formula to the single-phase-lagging heat conduction model. Few researchers [17-22] recently got the mathematical solutions of the fractional Cattaneo-Vernotte heat conduction problem with Neumann boundary conditions on a finite or semi-infinite medium. However, based on the Cattaneo-Vernotte fractional model, the heat conduction of the finite thickness along with the radiation

boundary condition has been less studied. Therefore, the analytical solution for the time-fractional heat conduction of Cattaneo in a finite thick plate under radiation conditions is studied in this paper. The heat conduction mechanism that differs from the fractional-order parameters is analyzed. The time-fractional thermoelastic analysis of the Cattaneo-type for a thick plate under radiation boundary conditions has not been investigated to the best of the author's knowledge.

The outline of the remaining paper is as follows. Section 2 presents the mathematical modeling of the generalized heat conduction equation in the framework of fractional Cattaneo-type, with its associated thermal stresses. Section 3 obtains the solution of time-fractional Cattaneo analysis under radiation conditions. Section 4 gives deduction and validation of the results. Section 5 gives outcomes that are graphically shown. Finally, conclusive comments are summarized in Section 6.

2. Mathematical Model
2.1 Fractional Cattaneo-Type Heat Conduction
The classical Cattaneo model [23] as

$$q + \tau \frac{\partial q}{\partial t} = -k \nabla T \tag{1}$$

By combining Eq. (1) with the continuity equation

$$\rho C_v \frac{\partial T}{\partial t} = -\nabla \cdot q \tag{2}$$

leads to the hyperbolic heat conduction equation

$$\frac{\partial T}{\partial t} + \tau \frac{\partial^2 T}{\partial t^2} = \kappa \Delta T \tag{3}$$

in which q is the heat flux vector, τ is the relaxation time, k is the heat conductivity of a solid, κ is the thermal diffusivity coefficient, ρ is the density, C_v is the calorific value, ∇ is the gradient operator, T is the temperature and t is the time, respectively.

The fractional generalization [24] of the classical Cattaneo model by introducing the fractional Taylor formula [21] as

$$q + \tau^p \frac{\partial^p q}{\partial t^p} = -k \nabla T, \, 0 < p \leq 1, \tag{4}$$

where without losing the generality $\Gamma(1+p)$ appearing in the Taylor series is merged in τ^p terms, Γ is the gamma function, p is introduced to keep the dimension in order and $\partial^p / \partial t^p$ is the fractional time derivative based on Caputo fractional definition [25]. For the limiting case of $\tau = 0$ (or $p=0$), Eq. (4) reduces to classical Fourier heat conduction and the standard Cattaneo heat conduction equation for $p=1$. The estimated ranges of relaxation time (in seconds) usually involve $(10^{-11} \square 10^{-14})$ for metals, $(10^{-8} \square 10^{-10})$ for gases, and $(10 \square 10^2)$ for porous materials [26].

Combining Eq. (4) with the law of conservation of energy shown in Eq. (2), leads to the fractional generalized Cattaneo equation as

$$\frac{\partial T}{\partial t} + \tau^p \frac{\partial^{p+1} T}{\partial t^{p+1}} = \kappa \Delta T, \, 0 < p \leq 1 \tag{5}$$

Taking the Laplace transform [27-29] of Eq. (4), one obtains

$$q^*(s) = -\frac{\kappa \nabla T^*(s)}{(1 + \tau^p s^p)}, \, 0 < p \leq 1 \tag{6}$$

in which the asterisk denotes the transform and s is a transform parameter. Using the inversion theorem of the Laplace transform, one gets the solution of Eq. (6) as

$$q(t) = -\frac{k}{\tau^p} \int_0^t (t-\gamma)^{p-1} E_{p,p} \left[-\frac{(t-\gamma)^p}{\tau^p} \right] \nabla T(\gamma) \, d\gamma \tag{7}$$

where $E()$ is the generalized Mittag-Leffler functions. Here Eq. (7) with $\tau^p = \zeta$ was obtained by Povstenko [13-15].

2.2 The Plate Under Radiation Boundary Conditions
Figure 1 shows a schematic sketch of the studied thermoelasticity problem and the cylindrical coordinate axes r, θ, z.
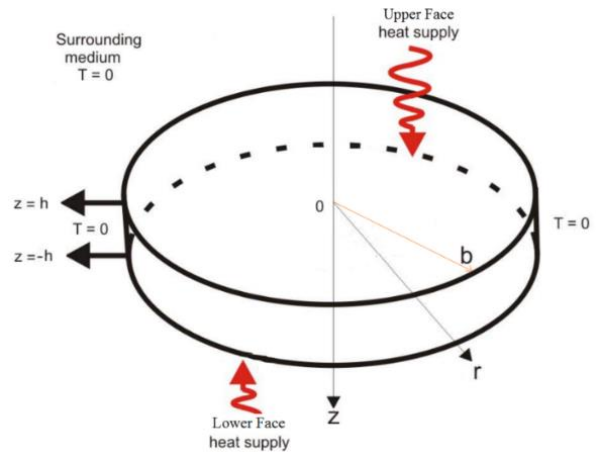

Figure 1 Plate configuration and heating conditions.

It is used to describe a time-fractional thermoelastic analysis of the thick plate under radiation boundary conditions. The two-dimensional finite thick circular plate occupies the domain $D = \{(r, z) \in [0, b] \times [-h, h]\}$ in the unstressed reference configuration. Equations governing the time-fractional Cattaneo-type heat conduction equation as

$$\frac{\partial T}{\partial t} + \tau^p \frac{\partial^{p+1} T}{\partial t^{p+1}} = \kappa \left[\frac{1}{r} \frac{\partial}{\partial r} \left(r \frac{\partial T}{\partial r} \right) + \frac{\partial^2 T}{\partial z^2} \right] + \chi(r, z, t),$$
$$0 \leq p \leq 1, 0 \leq r \leq b, -h \leq z \leq h, t > 0, \tag{8}$$

with zero initial condition

$$t = 0 : T = 0, \frac{\partial T}{\partial t} = 0, 0 \leq r \leq b, -h \leq z \leq h \tag{9}$$

under the Dirichlet-type boundary condition on the curved surface

$$r = b : T = 0, -h \leq z \leq h, \, t > 0, \tag{10}$$

where $T = T(r,z,t)$ is the temperature in cylindrical coordinates, $\kappa = k/(\rho C_v)$ is the thermal diffusivity of the material, k is the conductibility of the medium, ρ is its density, C_v is the calorific capacity, assumed to be constant, and $\chi(r,z,t)$ is the source function having physical dimension $[\chi] = {}^\circ\text{C}/\text{m}^2$, respectively.

Povstenko [30-32] has recently investigated the time-fractional heat conduction equation with Caputo derivative under mathematical and physical Robin-type boundary conditions. Another equivalent name in use is radiation-type boundary condition [33-37], a specification of a linear combination of the values of a temperature function and its normal derivative on the domain's boundary and can be given as $[\beta_i f + \alpha_i (\partial f / \partial z)]_{z=\pm h} = A_i(r,t)$ [36]. Here α_i and β_i $(i=1,2)$ are the constant thermal parameters related to the conduction and convection coefficients whose value can be positive, negative, or zero acting on surfaces $z = \pm h$ and $A_i (i=1,2)$ is temperature distributions of the surrounding media. As a particular case, these conditions of radiation-type contour acting on surfaces $z = -h$ and $z = h$ can be taken as

$$z = h \; : T + k_1 \frac{\partial T}{\partial z} = \xi \frac{\delta(r-r_0)}{r_0}\left(1 + \tau^p \frac{\partial^p}{\partial t^p}\right) f(t),$$

$$z = -h : T - k_2 \frac{\partial T}{\partial z} = \xi \frac{\delta(r-r_0)}{r_0}\left(1 + \tau^p \frac{\partial^p}{\partial t^p}\right) f(t),$$

(11)

where the radiation constant coefficients on the upper and lower surfaces are taken as $\beta_1 = \beta_2 = 1$, $\alpha_1 = k_1$, $\alpha_2 = k_2$ for a specified temperature on the boundary, ξ is the heat transfer coefficient having the physical dimension $[\xi] = {}^\circ\text{C}\,\text{m}$, $\delta(\;)$ is the Dirac delta function, $f(t) = H(t) - H(t-t_0)$ is the difference of two Heaviside functions, r_0 and t_0 is a fixed value, $H(\;)$ is the Heaviside function, and for the sake of brevity, we consider internal heat generation as

$$\chi(r,z,t) = Q_0 \frac{\delta(r-r_0)\,\delta(z)}{r_0} f(t),\; 0 \le r_0 \le b,$$

(12)

in which the coefficient Q_0 characterizes the stream of heat and has the physical dimension $[Q_0] = {}^\circ\text{C}\,\text{m}^2$.

2.3 Thermoelastic Formulation

The Navier's equations [38] without the body forces can be expressed as

$$\nabla^2 u_r - \frac{u_r}{r^2} + \frac{1}{1-2\upsilon}\frac{\partial e}{\partial r} - \frac{2(1+\upsilon)}{1-2\upsilon}\alpha_t \frac{\partial T}{\partial r} = 0,$$

$$\nabla^2 u_z - \frac{1}{1-2\upsilon}\frac{\partial e}{\partial z} - \frac{2(1+\upsilon)}{1-2\upsilon}\alpha_t \frac{\partial T}{\partial z} = 0,$$

(13)

where the displacement components in radial and axial directions are

$$u_r = \frac{\partial \varphi}{\partial r} - \frac{\partial^2 L}{\partial r \partial z},$$

$$u_z = \frac{\partial \varphi}{\partial z} + 2(1-\upsilon)\nabla^2 L - \frac{\partial^2 L}{\partial^2 z},$$

(14)

and the dilatation is

$$e = \frac{\partial u_r}{\partial r} + \frac{u_r}{r} + \frac{\partial u_z}{\partial z},$$

(15)

with α_t as the thermal expansion coefficient, υ represents Poisson's ratio, $L(r,z,t)$ is Love's function [37], and $\varphi(r,z,t)$ is Goodier's displacement potential that must satisfy the equation [38]

$$\nabla^2 \varphi = K_0 T,$$

(16)

and Love's function must satisfy the equation

$$\nabla^2 \nabla^2 L = 0,$$

(17)

where

$$K_0 = [(1+\upsilon)/(1-\upsilon)]\alpha_t.$$

(18)

The stress component [38] is

$$\sigma_{rr} = 2G\left\{\left(\frac{\partial^2 \varphi}{\partial r^2} - \nabla^2 \varphi\right) + \frac{\partial}{\partial z}\left[\upsilon\nabla^2 L - \frac{\partial^2 L}{\partial r^2}\right]\right\},$$

$$\sigma_{\theta\theta} = 2G\left\{\left(\frac{1}{r}\frac{\partial \varphi}{\partial r} - \nabla^2 \varphi\right) + \frac{\partial}{\partial z}\left[\upsilon\nabla^2 L - \frac{1}{r}\frac{\partial L}{\partial r}\right]\right\},$$

$$\sigma_{zz} = 2G\left\{\left(\frac{\partial^2 \varphi}{\partial z^2} - \nabla^2 \varphi\right) + \frac{\partial}{\partial z}\left[(2-\upsilon)\nabla^2 L - \frac{\partial^2 L}{\partial z^2}\right]\right\},$$

$$\sigma_{rz} = 2G\left\{\frac{\partial^2 \varphi}{\partial r \partial z} + \frac{\partial}{\partial r}\left[(1-\upsilon)\nabla^2 L - \frac{\partial^2 L}{\partial z^2}\right]\right\},$$

(19)

in which G is the shear modulus, υ is Poisson's ratio, and the Laplacian operator as

$$\nabla^2 = \frac{\partial^2}{\partial r^2} + \frac{1}{r}\frac{\partial}{\partial r} + \frac{\partial^2}{\partial z^2}.$$

(20)

The traction-free boundary conditions can be represented as follows:

$$r = b : \sigma_{rr} = \sigma_{rz} = 0,$$

(21)

and the other boundary conditions on the lower and upper surfaces are set free. Eqs. (8) to (21) constitute the mathematical formulation of the problem.

3. Solutions For The Plate Under Radiation Conditions
3.1 Solution Of Time-Fractional Cattaneo Analysis

Firstly, introducing the Hankel integral transform [39] and its inversion theorem as

$$T_n\{f(r)\} = f_{(r)}^{(\,)} = \int_0^b r\,J_0(\beta_n\,r)\,f(r)\,dr,$$
$$f(r) = \sum_n f_{(n)}^{(\,)}\,k_0(\beta_n\,r), \tag{22}$$

where n be the transform parameter and the kernel for the finite transform defined by

$$k_0(\beta_n\,r) = \frac{2}{b^2}\left[\frac{J_0(\beta_n\,r)}{\beta_n J_1^2(\beta_n\,b)}\right], \tag{23}$$

with β_n are the positive roots of the characteristic equation $J_0(\beta b) = 0$. We recall another integral transform proposed by Marchi and Fasulo [36] that responds to the radiation boundary conditions given in Eq. (11) as

$$T_{P_n}[g(z)] = g_{(z)}^{(\,)} = \int_{-h}^{h} g(z)P_m(z)\,dz,$$
$$g(z) = \sum_m \frac{g_{(m)}^{(\,)}}{\lambda_m}P_m(z), \tag{24}$$

where the orthogonal function gives the nucleus as

$$P_m(z) = Q_m\cos(a_m z) - W_m\sin(a_m z),$$
$$Q_m = a_m(k_2 + k_1)\cos(a_m h),$$
$$W_m = 2\cos(a_m h) + (k_2 - k_1)a_m\sin(a_m h), \tag{25}$$
$$\lambda_m = \int_{-h}^{h} P_m^2(z)\,dz = h\,[Q_m^2 + W_m^2] + \frac{\sin(2a_m h)}{2a_m}[Q_m^2 - W_m^2].$$

and the eigenvalues a_m are the positive roots of the characteristic equation

$$[k_1 a\cos(ah) + \sin(ah)]\,[\cos(ah) + k_2 a\sin(ah)] =$$
$$[k_2 a\cos(ah) - \sin(ah)]\,[\cos(ah) - k_1 a\sin(ah)]. \tag{26}$$

Following the rules defined in Eq. (22) and (24) to equation (8), one obtains

$$\left(\frac{d}{dt} + \tau^p\frac{d^{p+1}}{dt^{p+1}}\right)T_{(n,m,t)}^{(2)} + \kappa\Lambda T_{(n,m,t)}^{(2)} = H_{n,m}\,f(t), \tag{27}$$

subjected to the transformed initial condition (9) as

$$t = 0 : T_{(n,m,t)}^{(2)} = 0,\; \frac{\partial}{\partial t}T_{(n,m,t)}^{(2)} = 0, \tag{28}$$

where

$$\Lambda = a_m^2 + \beta_n^2, \tag{29}$$

$$H_{n,m} = \left\{\left[\frac{P_m(h)}{k_1} - \frac{P_m(-h)}{k_2}\right]\xi + Q_0 P_m(z)\right\}k(\beta_n r_0). \tag{30}$$

Then, the transformed temperature of Eq. (27) in the Laplace domain is

$$T_{(n,m,s)}^{(3)} = H_{n,m}\,T_{(s)}^{(3)}, \tag{31}$$

where

$$T_{(n,m,s)}^{(3)} = \int_0^\infty T_{(n,m,t)}^{(2)}\,e^{-st}\,dt,\quad F(s) = \int_0^\infty f(t)\,e^{-st}\,dt, \tag{32}$$

and

$$T_{(s)}^{(3)} = \frac{F(s)}{\kappa(s + \tau^p s^{1+p}) + \Lambda}. \tag{33}$$

Eq. (33) is expanded into the following form [21]

$$T_{(s)}^{(3)} = \sum_{l=0}^{\infty}(-1)^l\frac{\Lambda^{2l}\tau^{-(l+1)p}s^{-(l+1)}}{\kappa(s^p + \tau^{-p})^{l+1}}. \tag{34}$$

Applying the convolution theorem, the inversion of Laplace transforms for Eq. (34)

$$T_{(n,m,t)}^{(2)} = H_{n,m}\,k(\beta_n r_0)\int_0^t T_{(\eta)}^{(2)}f(t-\eta)d\eta. \tag{35}$$

By adopting the discretization method [40], one obtains

$$\begin{aligned}T_{(t)}^{(2)} &= L^{-1}\{T_{(s)}^{(3)}\} = L^{-1}\left\{\sum_{l=0}^{\infty}(-1)^l\frac{\Lambda^{2l}\tau^{-(l+1)p}s^{-(l+1)}}{\kappa(s^p + \tau^{-p})^{l+1}}\right\}\\ &= \sum_{l=0}^{\infty}(-1)^l\frac{\Lambda^{2l}\tau^{-(l+1)p}t^{l(p+1)+p}}{\kappa\,l!}E_{p,1+p+l}^{(l)}\left(-\frac{t^p}{\tau^p}\right),\end{aligned} \tag{36}$$

where $E_{\alpha,\beta}^{(l)}$ is the generalized Mittag-Leffler functions [26]

$$E_{\alpha,\beta}^{(l)}(z) = \frac{d^n}{dz^n}E_{\alpha,\beta}(z) = \sum_{j=0}^{\infty}\frac{(j+n)!z^j}{j!\,\Gamma(\alpha j + \alpha n + \beta)}. \tag{37}$$

Applying the inversion theorems of transformation rules defined in Eqs. (22) and (24) on equation (35), one obtains

$$T(r,z,t) = \sum_{n=1}^{\infty}\sum_{m=1}^{\infty}\wp_{n,m}\left\{\int_0^t T_{(\eta)}^{(2)}f(t-\eta)d\eta\right\}P_m(z)k(\beta_n r), \tag{38}$$

where

$$\wp_{n,m} = H_{n,m}\,k(\beta_n r_0)/(\lambda_m\Lambda). \tag{39}$$

Thus, Eq. (38) represents the temperature at every instant of the time-fractional Cattaneo heat conduction model and at all points of a thick circular plate when there are radiation-type conditions. Substituting the expression (31) into Eq. (16), one obtains Goodier's potential as

$$\varphi(r,z,t) = -K_0\sum_{n=1}^{\infty}\sum_{m=1}^{\infty}\frac{\wp_{n,m}}{\Lambda}\left\{\int_0^t T_{(\eta)}^{(2)}f(t-\eta)d\eta\right\}P_m(z)k_0(\beta_n r). \tag{40}$$

Similarly, Eq. (31) satisfying Eq. (17), one gets Love's function as

$$
L(r,z,t) = -K_0 \sum_{n=1}^{\infty} \sum_{m=1}^{\infty} \frac{\wp_{n,m}}{\Lambda} \left\{ \int_0^t T_{(\eta)}^{(2)} f(t-\eta) d\eta \right\} \cosh(\beta_n z)
$$
$$
\times [A_n J_0(\beta_n r) + C_n(\beta_n r) J_1(\beta_n r)], \tag{41}
$$

in which unknown arbitrary functions A_n and C_n are to be determined later. Using Eqs. (21) and (22) into Eq. (14), one obtains

$$
u_r = K_0 \sum_{n=1}^{\infty} \sum_{m=1}^{\infty} \frac{\wp_{n,m}}{\Lambda} \left\{ \int_0^t T_{(\eta)}^{(2)} f(t-\eta) d\eta \right\} \{ \beta_n \sinh(\beta_n z)
$$
$$
\times [A_n(-\beta_n) J_1(\beta_n r) + C_n \beta_n(\beta_n r) J_0(\beta_n r)] + (2/b^2)
$$
$$
\times [J_1(\beta_n r)/J_1(\beta_n b)] p_m(z) \}, \tag{42}
$$

$$
u_z = K_0 \sum_{n=1}^{\infty} \sum_{m=1}^{\infty} \frac{\wp_{n,m}}{\Lambda} \left\{ \int_0^t T_{(\eta)}^{(2)} f(t-\eta) d\eta \right\} \{ a_m [Q_m \sin(a_m z)
$$
$$
+ W_m \cos(a_m z)] k_0(\beta_n r) + A_n \beta_n^2 J_0(\beta_n r)(4\upsilon-3)
$$
$$
\times \cosh(\beta_n z) + C_n \beta_n^2 [4(1-\nu) J_0(\beta_n r) + (\beta_n r) J_1(\beta_n r)
$$
$$
\times (4\upsilon-3)] \cosh(\beta_n z) \}, \tag{43}
$$

The stress components were evaluated using Eqs. (19)-(21) in (19)

$$
\sigma_{rr} = -2G K_0 \sum_{n=1}^{\infty} \sum_{m=1}^{\infty} \frac{\wp_{n,m}}{\Lambda} \left\{ \int_0^t T_{(\eta)}^{(2)} f(t-\eta) d\eta \right\}
$$
$$
\times \left\{ \left[a_m^2 J_0(\beta_n r) - \beta_n \left(\frac{J_1(\beta_n r)}{r} \right) \right] \left(\frac{2}{b^2 \beta_n J_1(\beta_n b)} \right)
$$
$$
\times P_m(z) + \beta_n^3 C_n [(2\nu-1) J_0(\beta_n r) + (\beta_n r) J_1(\beta_n r)]
$$
$$
\times \sinh(\beta_n z) + \beta_n^2 A_n \left[\beta_n J_0(\beta_n r) - \frac{J_1(\beta_n r)}{r} \right] \sinh(\beta_n z) \right\}, \tag{44}
$$

$$
\sigma_{\theta\theta} = -2G K_0 \sum_{n=1}^{\infty} \sum_{m=1}^{\infty} \frac{\wp_{n,m}}{\Lambda} \left\{ \int_0^t T_{(\eta)}^{(2)} f(t-\eta) d\eta \right\}
$$
$$
\times \left\{ \left[\beta_n \left(\frac{J_1(\beta_n r)}{r} \right) - \Lambda J_0(\beta_n r) \right] \left(\frac{2}{b^2 \beta_n J_1(\beta_n b)} \right)
$$
$$
\times P_m(z) + \beta_n^2 A_n \sinh(\beta_n z) \left(\frac{J_1(\beta_n r)}{r} \right) \sinh(\beta_n z)
$$
$$
+ \beta_n^3 C_n(2\nu-1) J_0(\beta_n r) \sinh(\beta_n z) \right\}, \tag{45}
$$

$$
\sigma_{zz} = -2G K_0 \sum_{n=1}^{\infty} \sum_{m=1}^{\infty} \frac{\wp_{n,m}}{\Lambda} \left\{ \int_0^t T_{(\eta)}^{(2)} f(t-\eta) d\eta \right\}
$$
$$
\times \left\{ \frac{2}{b^2} \frac{\beta_n J_0(\beta_n r)}{J_1(\beta_n b)} P_m(z) - \beta_n^3 A_n J_0(\beta_n r) \sinh(\beta_n z) + \beta_n^3 C_n
$$
$$
\times [2(2-\nu) J_0(\beta_n r) - (\beta_n r) J_1(\beta_n r)] \sinh(\beta_n z) \right\}, \tag{46}
$$

$$
\sigma_{rz} = -2G K_0 \sum_{n=1}^{\infty} \sum_{m=1}^{\infty} \frac{\wp_{n,m}}{\Lambda} \left\{ \int_0^t T_{(\eta)}^{(2)} f(t-\eta) d\eta \right\} \{ -a_m [W_m \cos(a_m z)
$$
$$
+ Q_m \sin(a_m z)] \frac{2}{b^2} \frac{J_1(\beta_n r)}{J_1(\beta_n b)} + \beta_n^3 A_n J_1(\beta_n r) \cosh(\beta_n z)
$$
$$
- \beta_n^3 C_n [2(1-\nu) J_1(\beta_n r) + (\beta_n r) J_0(\beta_n r)] \cosh(\beta_n z) \}. \tag{47}
$$

Using Eqs. (21), (44) and (47), one obtains

$$
A_n = \frac{2\{[2(1-\nu)\beta_n] \mathrm{csch}(\beta_n z) P_m(z) + (\beta_n b) \mathrm{sech}(\beta_n z) P_m'(z)\}}{(\beta_n^2 b)^2 J_1(\beta_n b)\{1 - \beta_n^2 + \beta_n [b - 2(1-\nu)/b]\}},
$$
$$
C_n = \frac{2[-\beta_n \mathrm{csch}(\beta_n z) P_m(z) + \mathrm{sech}(\beta_n z) P_m'(z)]}{(\beta_n^2 b)^2 J_1(\beta_n b)[\beta_n^2 b - 2(1-\nu)]}. \tag{48}
$$

where prime denotes the differentiation of the function.

3.2 Solution Of The Classical Cattaneo-Vernotte Model

Taking $p = 1$, Eq. (8) can be reduced to Cattaneo-Vernotte heat conduction model as

$$
\kappa \left(\frac{\partial T}{\partial t} + \tau \frac{\partial^2 T}{\partial t^2} \right) = \frac{1}{r} \frac{\partial}{\partial r} \left(r \frac{\partial T}{\partial r} \right) + \frac{\partial^2 T}{\partial z^2} + \chi(r,z,t),
$$
$$
0 \leq r \leq b, -h \leq z \leq h, t > 0. \tag{49}
$$

Following the procedure in subsection 3.1, the solution of Eq. (49) can be obtained as

$$
T(r,z,t) = \sum_{n=1}^{\infty} \sum_{m=1}^{\infty} \wp_{n,m} \left\langle \frac{1}{2\Lambda\sqrt{1-4\tau\Lambda}} \exp\left[-\frac{(t-t_0)(1+\sqrt{1-4\tau\Lambda})}{2\tau} \right] \right.
$$
$$
\times \left\{ -1 + \exp\left[\frac{(t-t_0)(1+\sqrt{1-4\tau\Lambda})}{2\tau} \right](1 - 2\sqrt{1-4\tau\Lambda})
$$
$$
+ \exp\left[\frac{(t-t_0)(1+\sqrt{1-4\tau\Lambda})}{\tau} \right](1 + \sqrt{1-4\tau\Lambda}) \right\} H(t-t_0) \right\rangle
$$
$$
\times P_m(z) k_0(\beta_n, r). \tag{50}
$$

3.3 Solution Of The Fourier Heat Conduction Model

Taking $\tau = 0$, Eq. (8) can be reduced to the classical Fourier conduction model as

$$
\kappa \frac{\partial T}{\partial t} = \frac{1}{r} \frac{\partial}{\partial r} \left(r \frac{\partial T}{\partial r} \right) + \frac{\partial^2 T}{\partial z^2} + \chi(r,z,t),
$$
$$
0 \leq r \leq b, -h \leq z \leq h, t > 0. \tag{51}
$$

Following the procedure in subsection 3.1, the solution of Eq. (51) can be obtained as

$$
T(r,z,t) = \sum_{n=1}^{\infty} \sum_{m=1}^{\infty} \wp_{n,m} \left\langle (\exp[-\Lambda(t-t_0)] - 1) H(t-t_0) \right\rangle
$$
$$
\times P_m(z) k_0(\beta_n, r). \tag{52}
$$

4. Numerical Results, Discussion And Remarks

To interpret the numerical computations, we consider the material properties of Aluminum metal, which can be commonly used in both wrought and cast forms. In the following calculation, the physical parameters taken are $b = 1$, $h = 0.8$, $k_1 = k_2 = 0.86$ and $T_0 = 150$°C. The time, coordinate, displacement and stresses are normalized as follows

$$
\bar{r} = r/b, \ \bar{z} = [z - (-h/2)]/b, \ \bar{t} = \kappa t/b^2, \bar{\tau} = \kappa \tau/b^2,
$$
$$
\bar{T} = T/T_0, \ \bar{u}_i = u_i/K_0 T_0 b, \bar{\sigma}_{ij} = \sigma_{ij}/E\alpha T_0 \ (i,j = r,z), \tag{53}
$$

and (k_i, ξ, Q_0) is also taken into account when introducing nondimensional quantities for numerical calculation. The numerical results with various values of the fractional parameter p and the relaxation time $\bar{\tau}$ are taken between 0 to 10. The thermomechanical properties [34] of isotropic material at room temperature are considered in Table 1.

Table 1. Thermo-mechanical properties: Aluminum.

Dimension	Value
Modulus of Elasticity, E	68 GPa
Poisson's ratio	0.35
Thermal Expansion Coeff., α_t	$25.5 \times 10^{-6}/{}^0\text{C}$
Thermal diffusivity, κ	$84.18 \times 10^{-6} \text{ m}^2\text{s}^{-1}$
Thermal conductivity, λ	$204.2 \text{Wm}^{-1}\text{K}^{-1}$
Shear modulus, G	27 GPa
Density, ρ	2,710 Kg/m^3
Specific heat capacity, Cv	921.096 J/kg-K

Figures 2 and 3 represent the temperature distributions along radial and thickness directions for the thick plate with $\bar{r}_0 = 0.5$, $\bar{z}_0 = 0.5$, $\bar{t}_0 = 0.5$ and $\bar{t} = (0.1, 0.3, 0.5, 0.9, 1.2)$. Figure 2 shows that the temperature decreases when the dimensionless radial position is less than 0.5 inspite of an increase in the time value, which might be due to internal energy availability. The temperature increases up to 0.8 and again attains zero at the right boundary. The small temperature bump represents the absorption of heat from the external source. However, the area integral of the temperature distribution along the thickness direction shows a grown temperature bump and follows the standard bell-shaped curve irrespective of time variation. Figure 3 shows the dimensionless temperature profile for different values of the fractional-order p when $\bar{t} = 0.6$ is fixed. It shows that the tensile force is high at the left boundary, which reduces as it approaches the right edge. The maximum tensile strength is central in the thickness direction, with both ends having high compressive force, as shown in Figure 5. It can be seen in Figures 6 and 7 that the temperature distribution on the heated surface increases as time proceeds. The increment in temperature trend with a rise in fractional-order parameter and relaxation time is seen in Figures 6 and 7. In Figures 8 and 9 show the results for the thermal radial stress $\bar{\sigma}_{rr}$ for the different parameter values of p. Figure 8 shows that the maximum value of compressive stresses occurs up to $\bar{r} = 0.46$ along the radial direction, and the tensile stress acts towards the end. Figure 9 shows that the tensile stresses are maximum at the central part of thickness which is later overlaid by the compressive stress at both ends along the thickness direction. Figures 10 through 13 show the effects of fractional order p on tangential stress and axial direction. Initially, high tensile stress is noticed on the left boundary along the radial direction, as shown in Figures 10 and 12, which further show damping sine wave-like characteristics by attaining the minimum value. Figures 11 and 13 show a bimodal distribution along the thickness direction. Figures 14 and 15 display the dimensionless shear stress profile at different fractional-order parameters along the radial and thickness directions. Figure 14 shows that the maximum values of shear stresses occur on the plate's left boundary along the radial direction, which pretends as a damped sinusoidal function whose magnitude approaches zero as the radius position increases. In Figure 15, it is noted that the fluctuation occurs along the thickness direction.
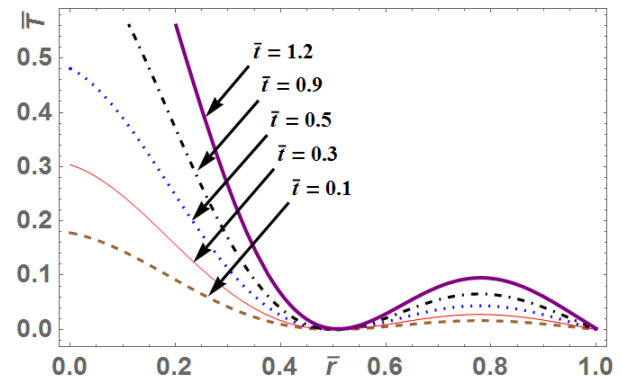

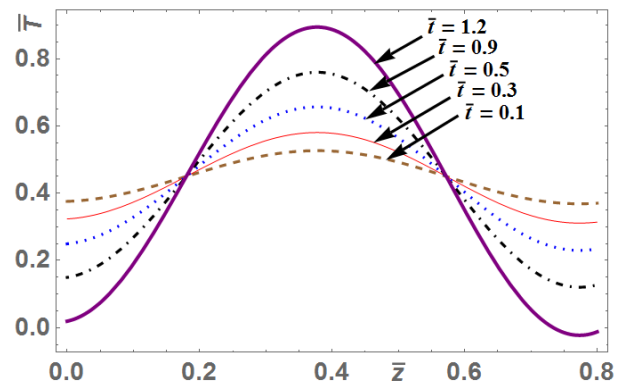Figure 2. Temperature profile at a different time when $p = 0.8$ along the $\bar{r}$ − direction.

Figure 3. Temperature profile at a different time when $p = 0.8$ along the $\bar{z}$ − direction.
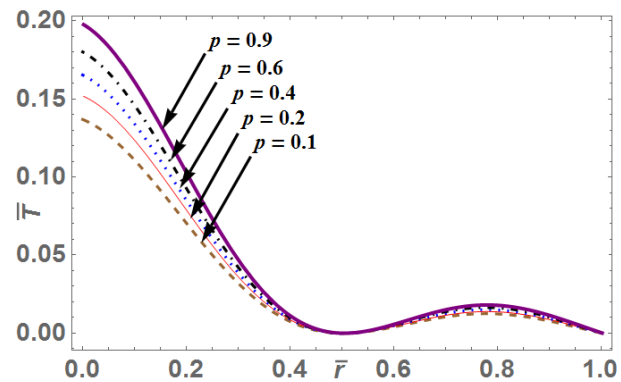

Figure 4. Temperature variation at various p when $\bar{t} = 0.6$ along the $\bar{r}$ − direction.
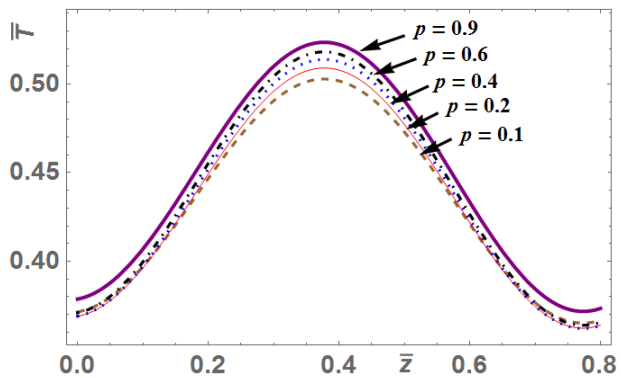

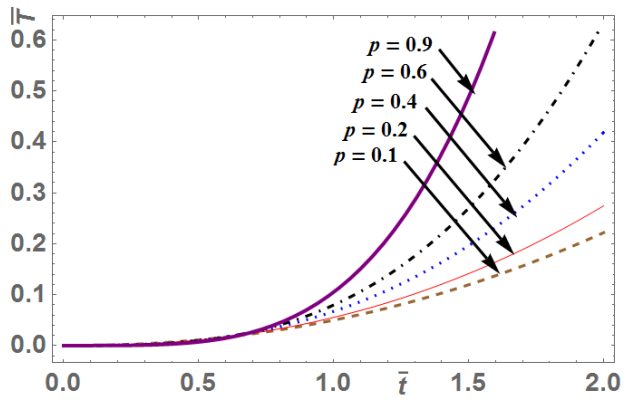Figure 5. Temperature variation at various p when $\bar{t} = 0.6$ along the $\bar{z}$ − direction.

Figure 6. Temperature distribution along dimensionless time at various p when $\tau = 0.6$.
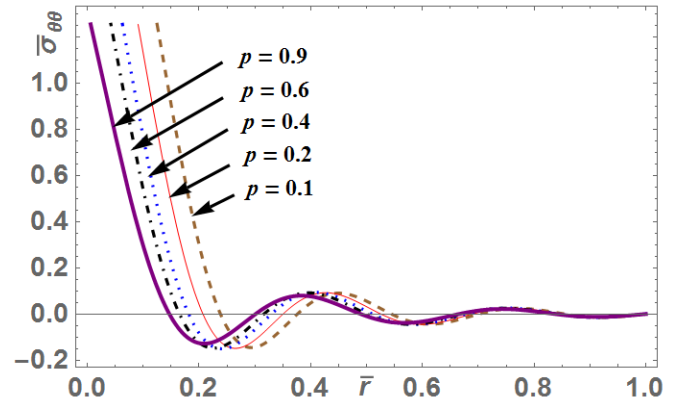

Figure 10. Effects of fractional order p on tangential stress along the $\bar{r}-$ direction.
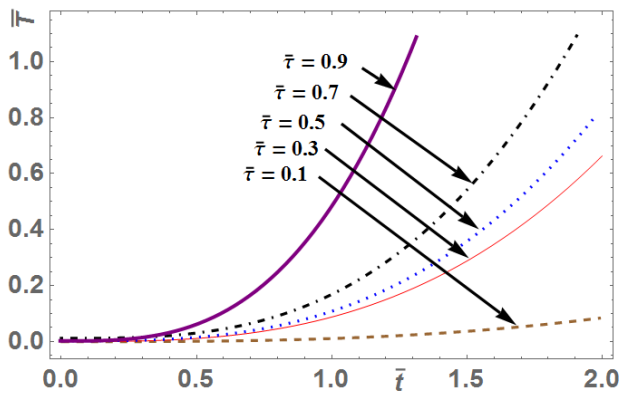

Figure 7. Temperature distribution along the time at various τ when $p = 0.6$ is fixed.
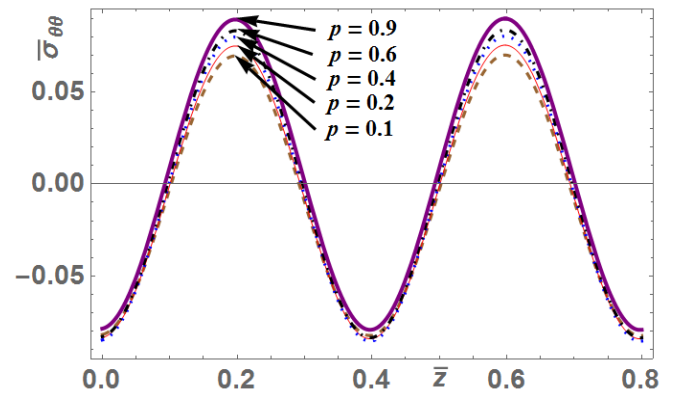

Figure 11. Effects of fractional order p on tangential stress along the $\bar{z}-$ direction.
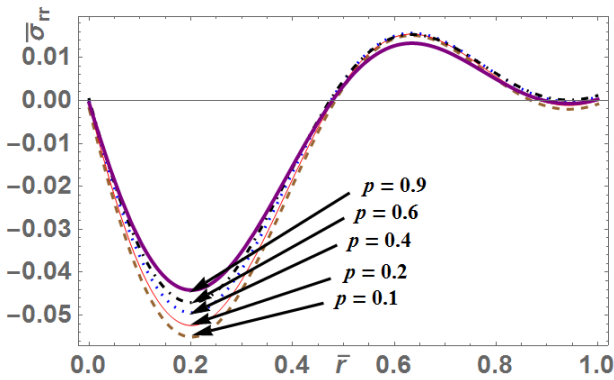

Figure 8. Radial stress profile at a different fractional order p along the $\bar{r}-$ direction.
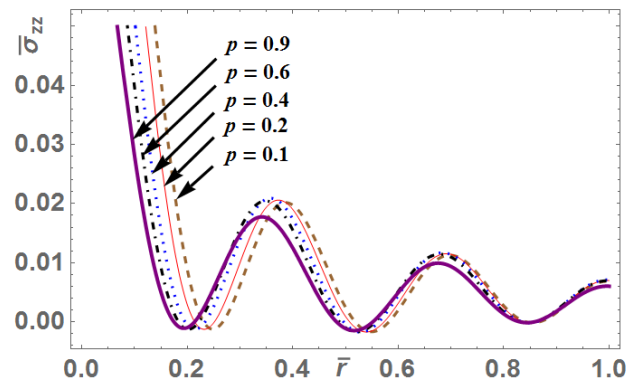

Figure 12. Dimensionless axial stress variation at a different p along the $\bar{r}-$ direction.
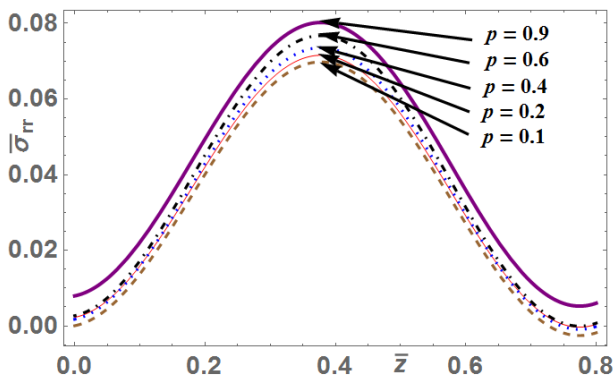

Figure 9. Radial stress profile at a different fractional order p along the $\bar{z}-$ direction.
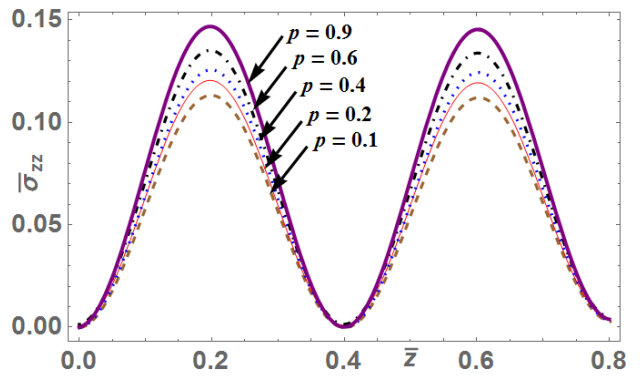

Figure 13. Dimensionless axial stress variation at a different p along the $\bar{z}-$ direction.
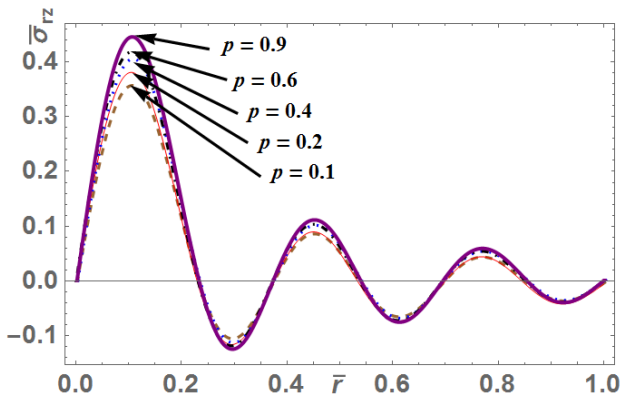
Figure 14. Shear stress distribution at different p along the $\bar{r}$ − direction.
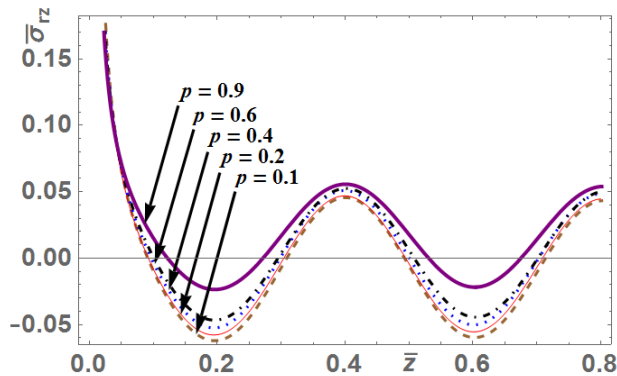

Figure 15. Shear stress distribution at different p along the $\bar{z}$ − direction.
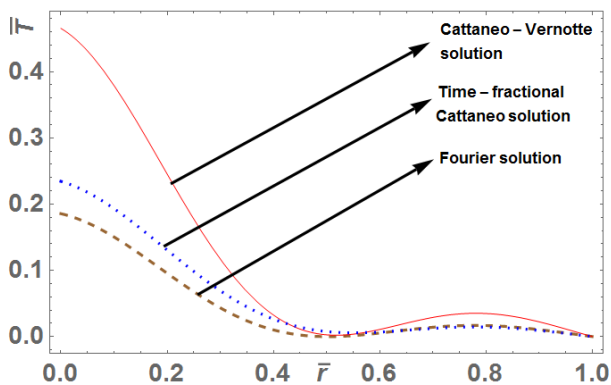

Figure 16. Comparing classical Cattaneo-Vernotte, fractional-order Cattaneo and Fourier models along the $\bar{r}$ − direction.
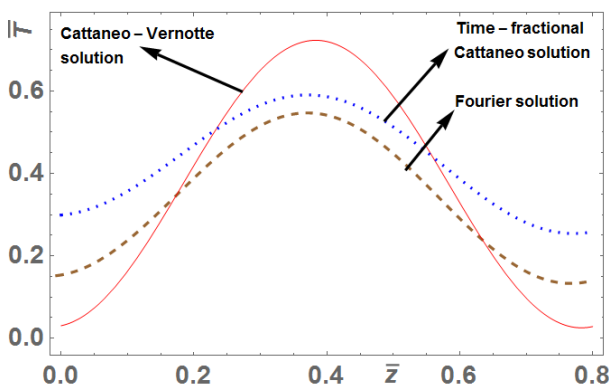

Figure 17. Comparing classical Cattaneo-Vernotte, fractional-order Cattaneo and Fourier models along the $\bar{z}$ − direction.

Figures 16 and 17 show the dimensionless temperature distribution profile compared to the classical Cattaneo-Vernotte, fractional-order Cattaneo and Fourier model fractional-order parameters along the radial and thickness direction. Figure 16 shows that the temperature field's maximum values occur on the plate's left boundary, whose magnitude approaches zero along the radial direction. Figure 17 shows that the temperature distribution along the thickness direction depicts a normal bell-shaped curve bump for all three model solutions.

4. Deduction And Validation Of The Results

This section refers to the deduction of the conclusions derived in the previous section regarding the classical uncoupled thermoelasticity model and the classical Cattaneo-Vernotte thermoelasticity theory for a homogeneous thick plate

(i) Taking $p = 1$ in Eq. (5), the equation results in the classical Cattaneo-Vernotte heat conduction model [24] as given in Eq. (49) with a solution in Eq. (50).
(ii) Taking $\tau = 0$ in Eq. (5), the equation reduces to the classical Fourier heat conduction model [41] as given in Eq. (51) with a solution in Eq. (52).

The key that was derived by Deshmukh et al. [41] for an isotropic, homogeneous, elastic hollow is compatible with the present thermoelastic solutions that were determined. In this piece of research, a fractional-order constitutive model and the classic continuity equation are brought together. Recent research [47,48] shows that it is possible for a non-Fourier constitutive model and a non-trivial continuity equation based on the Boltzmann transport theory to coexist. The findings demonstrate that the constitutive model and the continuity equation are not independent of one another, which is something that this work does not take into consideration.

5. Conclusion

In this problem, the fractional Cattaneo model is derived for studying the thermoelastic response for a finite thick circular plate impacted by an assigned temperature. At the same time, heat supply appears as a source in the energy equation. The integral transformation theory is used to obtain the analytical solution for the fractional Cattaneo and classical Fourier models. The temperature distribution dependence and its thermoelastic response on the fractional-order parameter and relaxation time are studied for different times and positions. It is observed that the fractional Cattaneo model gives continuous temperature and thermal stress variation irrespective of the fractional-order parameter. It is also detected that the heat flux flows from higher temperatures to lower for the fractional Cattaneo and classical Fourier models. Based on the findings of this study, we have come to the following conclusions:

1. The fractional parameter does have a substantial impact on the various components. Somewhere along the line, the fractional parameter will cause the variations to move in the opposite direction. In contrast, in other places, it will cause the amplitude of the variation to shift.
2. When looking at the stress component, the conductive temperature, the temperature change, and the cubic dilatation components, it is observed that the pattern of changes consists of rapid descents and jumps.

3. As the variations are studied, the thermal stress function, the stress components, and the smooth face either grow or decrease.

4. In the future, it will be possible to build such a mathematical model for a transversely isotropic media, and then it will be possible to investigate the changes.

5. Those who are engaged in studying thermodynamics and thermoelasticity will find this model to be of great assistance to them.

6. The solution to the problem can be applied to a two-dimensional problem with a dynamic response caused by a variety of thermal sources; this solution has a number of geophysical and industrial applications.

Nomenclature:

α_t linear coefficient of thermal expansion $(/^0C)$
κ thermal diffusivity $(m^2 s^{-1})$
k thermal conductivity $(W/m.K)$

Greek symbols
μ Lame's constants (GPa)
v Poisson's ratio
ρ density (kg/m3)
σ_{ij} components of stress tensor

References:

[1] M. Haskul, "Elastic state of functionally graded curved beam on the plane stress state subject to thermal load," *Mech. Based Des. Struct. Mach.*, 48 (6), 739-754, 2020. DOI: 10.1080/15397734.2019.1660890.

[2] E. Arslan, M. Haskul, "Generalized plane strain solution of a thick-walled cylindrical panel subjected to radial heating," *Acta Mech*, 226, 1213–1225, 2015. https://doi.org/10.1007/s00707-014-1248-4

[3] M. Haskul, E. Arslan and W. Mack, "Radial heating of a thick-walled cylindrically curved FGM-panel," *Z. Angew. Math. Mech.*, 97, 309-321, 2017. https://doi.org/10.1002/zamm.201500310

[4] M. Haskul, "Yielding of functionally graded curved beam subjected to temperature," *Pamukkale University Journal of Engineering Sciences*, 26 (4), 587-593, 2020. DOI: 10.5505/pajes.2019.92331

[5] E. Hoashi, T. Yokomine, A. Shimizu, and T. Kunugi, "Numerical analysis of wave-type heat transfer propagating in a thin foil irradiated by short-pulsed laser," *Int. J. Heat Mass Transf.*, 46 (19), 4083–4095, 2003. DOI: 10.1016/S0017-9310(03)00225-4.

[6] X. Ai and B. Q. Li, "Numerical simulation of thermal wave propagation during laser processing of thin films," *J. Electron. Mater.*, 34 (5), 583–591, 2005. DOI: 10.1007/s11664-005-0069-6.

[7] T. T. Lam and E. Fong, "Application of solution structure theorem to non-Fourier heat conduction problems: Analytical approach," *Int. J. Heat Mass Transf.*, 54, 4796–4806, 2011. DOI: 10.1016/j.ijheatmasstransfer.2011.06.028.

[8] T. T. Lam, "A unified solution of several heat conduction models," *Int. J. Heat Mass Transf.*, 56 (1–2), 653–666, 2013. DOI: 10.1016/j.ijheatmasstransfer.2012.08.055.

[9] C. Cattaneo, "Sur uneforme de l'équation de la chaleuréliminant le paradoxed'une propagation instantanée," *C. R. Acad. Sci.*, 247, 431–433, 1958.

[10] P. Vernotte, "Les paradoxes de la théorie continue de l'équation de la chaleur," *C. R. Acad. Sci.*, 246, 3154-3155, 1958.

[11] A. Compte and R. Metzler, "The generalized Cattaneo equation for the description of anomalous transport processes," *J. Phys. A: Math. Gen.*, 30, 7277-7289, 1997.

[12] F. M. Jiang, D. Y. Liu, and J. H. Zhou, "Non-Fourier heat conduction phenomena in porous material heated by microsecond laser pulse," *Microscale Thermophys. Eng.*, 6 (4), 331–346, 2003. DOI: 10.1080/10893950290098386.

[13] Y. Povstenko, *Fractional thermoelasticty*, Springer, New York, 2015.

[14] Y. Povstenko, "Fractional heat conduction equation and associated thermal stress," *J. Therm. Stresses*, 28 (1), 83–102, 2005.

[15] Y. Povstenko, "Fractional Cattaneo-type equations and generalized thermoelasticity," *J. Therm. Stresses*, 34 (2), 97-114, 2011. DOI: 10.1080/01495739.2010.511931.

[16] T. N. Mishra and K. N. Rai, "Numerical solution of FSPL heat conduction equation for analysis of thermal propagation," *Appl. Math. Comput.*, 273, 1006–1017, 2016. DOI: 10.1016/j.amc.2015.10.082.

[17] H. Qi, H. Xu, and X. Guo, "The Cattaneo-type time fractional heat conduction equation for laser heating," *Comput. Math. Appl.*, 66 (5), 824–831, 2013. DOI: 10.1016/j.camwa.2012.11.021.

[18] H. Qi, and X. Guo, "Transient fractional heat conduction with generalized Cattaneo model," *Int. J. Heat Mass Transf.*, 76, 535–539, 2014.

[19] H. Xu, H. Qi, and X. Jiang, "Fractional Cattaneo heat equation on a semi-infinite medium," *Chin. Phys. B*, 22 (1), 014401, 2013. DOI: 10.1088/1674-1056/22/1/014401.

[20] G. Xu, J. Wang, and Z. Han, "Study on the transient temperature field based on the fractional heat conduction equation for laser heating," *Appl. Math. Mech.*, 36, 844–849, 2015.

[21] G. Xu and J. Wang, "Analytical solution of time fractional Cattaneo heat equation for finite slab under pulse heat flux," *Appl. Math. Mech.*, 39 (10), 1465–1476, 2018. DOI: 10.1007/s10483-018-2375-8.

[22] G. Xu, J. Wang, and Z. Han, "Notes on 'The Cattaneo-type time fractional heat conduction equation for laser heating' [Comput. Math. Appl. 66 (2013) 824–831]," *Comput. Math. Appl.*, 71 (10), 2132–2137, 2016. DOI: 10.1016/j.camwa.2016.03.011.

[23] C. Cattaneo, "Sulla conduzione del calore," *Atti Sem. Mat. Fis. Univ. Modena*, 3, 83–101, 1948.

[24] H. R. Ghazizadeh, M. Maerefat, and A. Azimi, "Explicit and implicit finite difference schemes for

fractional Cattaneo equation," *J. Comput. Phys.*, 229 (16), 7042–7057, 2010. DOI: 10.1016/j.jcp.2010.05.039.

[25] Z. M. Odibat, N. T. Shawagfeh, "Generalized Taylor's formula," *Appl. Math. Comput.*, 186, 286–293, 2007.

[26] I. Podlubny, *Fractional Differential Equations*, Academic Press, New York, 1999.

[27] Z. Zhang and D.Y. Liu, "Advanced in the study of non-Fourier heat conduction," *Advance Mechanics*, 30, 446-456, 2000.

[28] R. Gorenflo and F. Mainardi, *Fractional Calculus: Integral and Differential Equations of Fractional Order*, A. Carpinteri and F. Mainardi (Editors): Fractals and Fractional Calculus in Continuum Mechanics), 223-276, Springer Verlag, Wien and New York, 1997.

[29] A. A. Kilbas, H. M. Srivastava, and J. J. Trujillo, *Theory and applications of fractional differential equations*, 204, Elsevier Science, Amsterdam, 2006.

[30] Y. Povstenko, "Axisymmetric Solutions to Time-fractional heat conduction equation in a half-space under Robin boundary conditions," *Int. J. Differ. Equ.*, 1–13, 2012. DOI: 10.1155/2012/154085.

[31] Y. Povstenko, "Axisymmetric solutions to fractional diffusion-wave equation in a cylinder under Robin boundary condition," *Eur. Phys. J. Spec. Top.*, 222, 1767–1777, 2013. DOI: 10.1140/epjst/e2013-01962-4.

[32] Y. Povstenko, "Fundamental solutions to the fractional heat conduction equation in a ball under Robin boundary condition," *Centr. Eur. J. Math.*, 12 (4), 611–622, 2014. DOI: 10.2478/s11533-013-0368-8.

[33] H. S. Carslaw and J.C. Jaeger, *Conduction of Heat in Solids*, 2nd ed., Oxford University Press, Oxford, 1959.

[34] G. M. L. Gladwell, J. R. Barber, and Z. Olesiak, "Thermal problems with radiation boundary conditions," *Q. J. Mech. Appl. Math.*, 36 (3), 387–401, 1983. DOI: 10.1093/qjmam/36.3.387.

[35] E. Marchi and G. Zgrablich, "Heat conduction in hollow cylinders with radiation," *Proc. Edimburgh Math. Soc.*, 14(11), 159-164, 1964.

[36] E. Marchi and A. Fasulo, "Heat conduction in sector of hollow cylinder with radiation," *Atti, della Acc. Sci. di. Torino*, 101, 373-382, 1967.

[37] R. Kumar, N. K. Lamba, and V. Varghese, "Analysis of thermoelastic disc with radiation conditions on the curved surfaces," *Mater. Phys. Mech.*, 16 (2), 175-186, 2013.

[38] N. Noda, R. B. Hetnarski, Y. Tanigawa, *Thermal stresses*, 2nd ed., Taylor and Francis, New York, 2003.

[39] A. E. H. Love, A Treatise on the mathematical theory of elasticity, 4th ed., Dover publications, New York, 1944.

[40] W. Nowacki, *Thermoelasticity*, 2nd ed., PWN-Polish Scientific Publishers, Warsaw and Pergamon Press, Oxford, 1986.

[41] J. J. Tripathi, K. C. Deshmukh and J. Verma, Fractional Order Generalized Thermoelastic Problem in a Thick Circular Plate with Periodically Varying Heat Source, *Int. J. Thermodyn.*, 20 (3), 132-138, 2017. DOI: 10.5541/ijot.5000190819.

[42] K. C. Deshmukh, S. D. Warbhe, and V. S. Kulkarni, "Brief Note on Heat Flow With Arbitrary Heating Rates in a Hollow Cylinder," *Therm. Sci.*, 15 (1), 275–280, 2011. DOI: 10.2298/TSCI100817063D.

[43] S. N. Li, B. Y. Cao, "Fractional Boltzmann transport equation for anomalous heat transport and divergent thermal conductivity," *Int. J. Heat Mass Transf.*, 137, 84-89, 2019. DOI: 10.1016/j.ijheatmasstransfer.2019.03.120.

[44] S. N. Li, B. Y. Cao, "Fractional-order heat conduction models from generalized Boltzmann transport equation," *Philos. Trans. R. Soc. A*, 378, 20190280, 2020. DOI: 10.1098/rsta.2019.0280.